



## ARTICLE

# CDER167, a dual inhibitor of URAT1 and GLUT9, is a novel and potent uricosuric candidate for the treatment of hyperuricemia

Ze-an Zhao<sup>1</sup>, Yu Jiang<sup>1</sup>, Yan-yu Chen<sup>1</sup>, Ting Wu<sup>1</sup>, Qun-sheng Lan<sup>1</sup>, Yong-mei Li<sup>1</sup>, Lu Li<sup>1</sup>, Yang Yang<sup>1</sup>, Cui-ting Lin<sup>1</sup>, Ying Cao<sup>1</sup>, Ping-zheng Zhou<sup>1</sup>, Jia-yin Guo<sup>1</sup>, Yuan-xin Tian<sup>1</sup> and Jian-xin Pang<sup>1</sup>

Urate transporter 1 (URAT1) and glucose transporter 9 (GLUT9) are important targets for the development of uric acid-lowering drugs. We previously showed that the flexible linkers of URAT1 inhibitors could enhance their potency. In this study we designed and synthesized CDER167, a novel RDEA3710 analogue, by introducing a linker (methylene) between the naphthalene and pyridine rings to increase flexibility, and characterized its pharmacological and pharmacokinetics properties *in vitro* and *in vivo*. We showed that CDER167 exerted dual-target inhibitory effects on both URAT1 and GLUT9: CDER167 concentration-dependently inhibited the uptake of [<sup>14</sup>C]-uric acid in URAT1-expressing HEK293 cells with an IC<sub>50</sub> value of 2.08 ± 0.31 μM, which was similar to that of RDEA3710 (its IC<sub>50</sub> value was 1.47 ± 0.23 μM). Using site-directed mutagenesis, we demonstrated that CDER167 might interact with URAT1 at S35 and F365. In GLUT9-expressing HEK293T cells, CDER167 concentration-dependently inhibited GLUT9 with an IC<sub>50</sub> value of 91.55 ± 15.28 μM, whereas RDEA3710 at 100 μM had no effect on GLUT9. In potassium oxonate-induced hyperuricemic mice, oral administration of CDER167 (10 mg·kg<sup>-1</sup>·d<sup>-1</sup>) for 7 days was more effective in lowering uric acid in blood and significantly promoted uric acid excretion in urine as compared with RDEA3710 (20 mg·kg<sup>-1</sup>·d<sup>-1</sup>) administered. The animal experiment proved the safety of CDER167. In addition, CDER167 displayed better bioavailability than RDEA3710, better metabolic stability and no hERG toxicity at 100 μM. These results suggest that CDER167 deserves further investigation as a candidate antihyperuricemic drug targeting URAT1 and GLUT9.

**Keywords:** gout; hyperuricemia; uric acid-lowering drugs; RDEA3710; CDER167; urate transporter 1 (URAT1); glucose transporter 9 (GLUT9)

*Acta Pharmacologica Sinica* (2022) 43:121–132; <https://doi.org/10.1038/s41401-021-00640-5>

## INTRODUCTION

Hyperuricemia is defined as a serum urate concentration >6.8 mg/dL [1] in the human body. High serum urate is associated with elevated body mass index [2], hypercholesterolemia [3], hypertriglyceridemia [4], increased fasting plasma glucose [5], and insulin resistance [6]. In addition, growing evidence has illuminated the dose effect of urate on the risk of metabolic syndrome [7], and an elevated urate level may have adverse cardiovascular effects [8]. Therefore, treatment of hyperuricemia is necessary. At present, excessive production of uric acid and insufficient excretion are the main causes of hyperuricemia. Over 90% of hyperuricemia is caused by insufficient uric acid excretion. Excretion of uric acid is dependent on urate transporters, such as urate transporter 1 (SLC22A12/URAT1) and glucose transporter 9 (SLC2A9/GLUT9). Therefore, URAT1 and GLUT9 have become important targets for the development of uric acid-lowering drugs.

To date, the uricosuric drugs used in the clinic mainly include benzbromarone, probenecid [9] and lesinurad [10]. Benzbromarone and probenecid can inhibit URAT1 and GLUT9 and thus

promote uric acid excretion. However, due to the fulminant hepatitis caused by benzbromarone [11], it has been withdrawn from the market in most countries. Because of low selectivity, probenecid can lead to drug-drug interactions [12], and therefore, its clinical use is limited. Lesinurad is a more selective URAT1 inhibitor developed by AstraZeneca and was approved by the FDA in October 2015 for the treatment of hyperuricemia [13], but it should be used in combination with a xanthine oxidase inhibitor (allopurinol/febuxostat). RDEA3710 is derived from lesinurad, which is currently in a phase II clinical trials [14]. Our previous experiments showed that the URAT1 inhibition activity of RDEA3710 was ~20 times that of lesinurad *in vitro* [15]. In addition to the abovementioned drugs, losartan, fenofibrate, atorvastatin and others also have a uric acid-lowering effect, but their mechanisms have not been fully elucidated. Studies have shown that losartan [16] can promote uric acid excretion and play a role in lowering uric acid by inhibiting GLUT9. However, no other new GLUT9 inhibitors have been reported, let alone drugs that inhibit both URAT1 and GLUT9. Therefore, it is of great significance to find new drugs to treat hyperuricemia.

<sup>1</sup>Guangdong Provincial Key Laboratory of Drug Screening, School of Pharmaceutical Sciences, Southern Medical University, Guangzhou 510515, China

Correspondence: Jia-yin Guo (g1227@smu.edu.cn) or Yuan-xin Tian (tyx523@163.com) or Jian-xin Pang (pjax@smu.edu.cn)

These authors contributed equally: Ze-an Zhao, Yu Jiang, Yan-yu Chen

Received: 17 November 2020 Accepted: 5 March 2021

Published online: 25 March 2021

In recent years, studies have shown that inserting a methylene unit between the triazole and naphthyridine of lesinurad can enhance its URAT1 inhibition activity [17]. Our group previously changed the 3 N atoms on the triazolium in lesinurad to C atoms and found that its activity increased nearly 20 times and its selectivity was 4 times greater than that of lesinurad. Recently, we also analyzed the contribution of flexible chains in URAT1 inhibitors by establishing hologram quantitative structure-activity relationship techniques (HQSAR) and topomer CoMFA models, both of which suggested that the linker between the two aromatic groups played a positive role in biological activity [18]. Therefore, based on the structure of RDEA3170, we inserted a methylene between the aromatic groups and named the new compound CDER167. Then, we predicted the activity of the compound using HQSAR. The predicted  $IC_{50}$  value ( $pIC_{50}$ ) was  $6.44 \mu\text{M}$ , which was lower than the actual  $IC_{50}$  value of lesinurad ( $7.18 \mu\text{M}$ ). In vitro studies revealed that  $10 \mu\text{M}$  CDER167 induced a significant reduction in the urate transport activity of URAT1. The present study aimed to evaluate the pharmacological effects of CDER167 compared with RDEA3170 in vitro and in vivo and the results showed that CDER167 was a better choice for the treatment of hyperuricemia.

## MATERIALS AND METHODS

### Materials

CDER167 is a light yellow powder with the molecular formula  $C_{21}H_{18}N_2O_2S$  ( $M_w$  362.45). Its structure and synthetic pathway are shown in Scheme 1, and the synthesis and characterization of CDER167 are presented in Supplementary Fig. S1. HPLC results showed that the purity of the compound was higher than 98%. RDEA3170 was purchased from HWRK Chemical Co., Ltd (Beijing, China). Uric acid, benzbromarone, allopurinol and probenecid were purchased from Sigma-Aldrich (St. Louis, MO, USA).  $[8-^{14}\text{C}]$  Uric acid ( $55 \text{ mCi/mmol}$ ) was purchased from American Radiolabeled

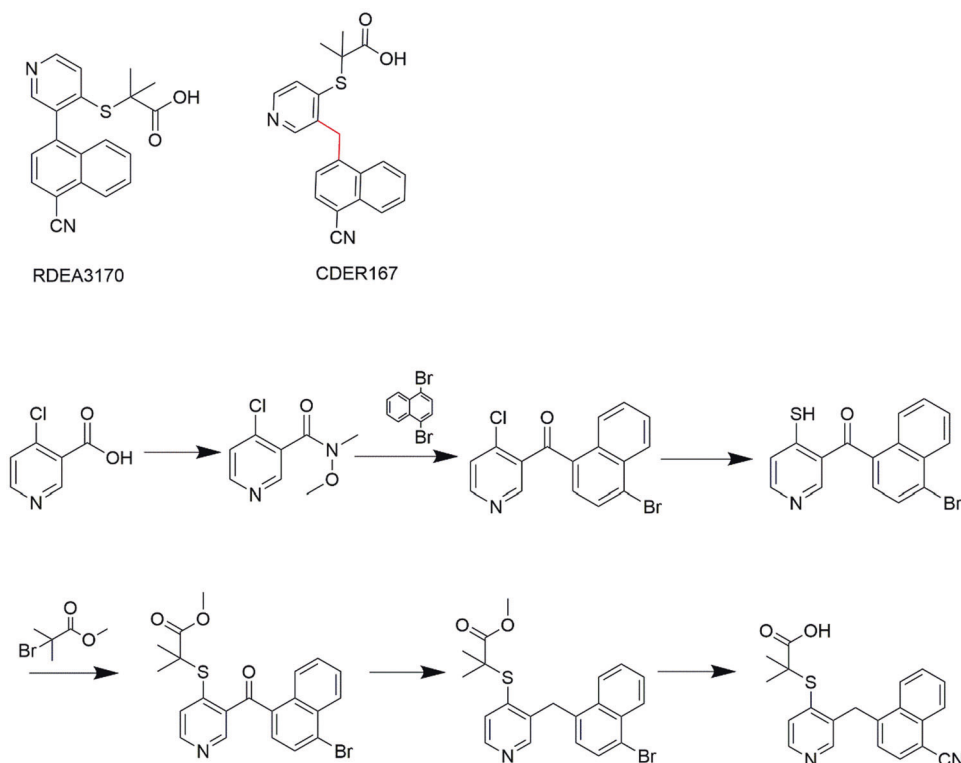
Chemicals (ARC, St. Louis, MO, USA). Potassium oxonate (PO) was obtained from Aladdin Reagent Co. (Shanghai, China). Uric acid, creatinine (CR) and urea nitrogen assay kits were purchased from BioAssay Systems (California, USA).

### Plasmid construction

The plasmids were constructed by Sangon, Inc. (Shanghai, China) and confirmed with a DNA sequencing analyzer (Applied Biosystems, Foster City, CA, USA). Plasmids expressing human URAT1 (gene ID: 116085, *Homo sapiens*) and ABCG2 (gene ID: 9429, *Homo sapiens*) were subcloned into a pcDNA3.1(+) vector, and mouse GLUT9 (gene ID: 117591, *Mus musculus* SLC2A9) was subcloned into a pcDNA3.1(-) vector. We used mouse GLUT9 instead of human GLUT9, as the recorded currents were larger in mGLUT9-transfected cells, which makes it easier to explore the efficacy of potent GLUT9 inhibitors [19].

### Cell culture and transfection

HEK293 cells were cultured in Dulbecco's modified Eagle's medium (DMEM, Gibco) supplemented with 10% fetal bovine serum and 1% penicillin-streptomycin in 24-well plates and incubated at  $37^\circ\text{C}$  with 5%  $\text{CO}_2$ . For better cell adhesion, poly-*D*-lysine ( $0.1 \text{ mg/mL}$ ) was incubated for 12 h in 24-well plates before seeding the cells. At 75%–85% confluence, HEK293 cells were cotransfected with plasmids expressing URAT1, ABCG2 or GLUT9 along with EGFP at a ratio of 2:1 using Lipofectamine 3000 (Invitrogen, Carlsbad, CA, USA). Then, 18–24 h after transfection, the fluorescent tag EGFP was used as a marker to ensure that the plasmid was successfully transfected into the cells. Successfully transfected cells expressing URAT1 and ABCG2 were used to perform  $[8-^{14}\text{C}]$  uric acid uptake assays, while cells expressing GLUT9 were split using trypsin-EDTA and replated onto 10 mm coverslips coated with  $0.1 \text{ mg/mL}$  poly-*D*-lysine (Sigma-Aldrich, Shanghai, China) for electrophysiology experiments.



**Scheme 1** The structure and the synthetic route of CDER167.

**[8-<sup>14</sup>C] Uric acid uptake assay of URAT1**

After transfection for 24 h, the culture medium was removed, and the cells were incubated with uric acid uptake buffer (containing 125 mM sodium gluconate, 4.8 mM potassium gluconate, 1.2 mM monobasic potassium phosphate, 1.2 mM magnesium sulfate, 1.3 mM calcium gluconate and 5.6 mM glucose) for 15 min. The uptake process was initiated by the addition of 25  $\mu$ M [8-<sup>14</sup>C] uric acid in the presence or absence of test compounds, such as RDEA3170, CDER167, benzbromarone and probenecid. Cells were then washed three times with ice-cold DPBS to terminate the reaction after 15 min. Next, 100  $\mu$ L of 0.1 M sodium hydroxide was added to lyse the cells. Intracellular radioactivity was determined with a liquid scintillation counter (PerkinElmer, Boston, MA, USA) after the addition of 1 mL of scintillant. Each experiment was performed in triplicate.

**Electrophysiological recordings of GLUT9 currents**

Electrophysiological recordings were conducted 18 h after transfection using the whole-cell patch-clamp technique and measured with a MultiClamp 700B patch-clamp amplifier/Digidata 1550B digitizer and pClamp 10 software (Molecular Devices, Sunnyvale, CA, USA), as previously reported by us [20].

**[8-<sup>14</sup>C] Uric acid uptake assay of ABCG2**

Membrane vesicles were prepared from HEK293-ABCG2 cells as reported [21]. In brief, cells were harvested and resuspended in ice-cold homogenization buffer (0.5 mM sodium phosphate, 0.1 mM EDTA, pH 7.4) containing protease inhibitors and shaken at 4 °C for 1 h. Then, lysed cells were centrifuged at 100,000  $\times$  *g* and 4 °C for 30 min, and the pellets were homogenized in ice-cold TS buffer (10 mM Tris-HEPES, 250 mM sucrose, pH=7.4). After centrifugation at 500  $\times$  *g* and 4 °C for 20 min, the supernatant was centrifuged at 100,000  $\times$  *g* and 4 °C for 60 min. The resulting pellet was resuspended in TS buffer.

Fifty microliters of membrane vesicle mixture containing 20  $\mu$ M [<sup>14</sup>C]-uric acid and 4 mM ATP was incubated with or without inhibitor for 15 min at 37 °C, and the reaction was started by adding 25  $\mu$ L of 10 mM ATP (or AMP for a background control). Five minutes later, the reaction was stopped by adding 200  $\mu$ L of ice-cold washing buffer, and this solution was added to a 0.45  $\mu$ m Ultrafree filter (Merck Millipore, Darmstadt, Germany). The filter was immediately centrifuged at 3000  $\times$  *g* for 20 s. Following two washing steps with ice-cold Hanks' balanced salt solution, the vesicles were solubilized by the addition of 200  $\mu$ L of 0.1 M NaOH. Radioactivity was determined with a liquid scintillation counter (PerkinElmer, Boston, MA, USA) after the addition of 0.5 mL of scintillant.

**Induction of hyperuricemia and drug administration**

SPF male Kunming mice weighing 18–20 g were obtained from the Laboratory Animal Centre of Southern Medical University (Guangzhou, China). They were given free access to food and water for at least 1 week to adapt to the environment before experiments and kept in a controlled light environment with 12 h of light and 12 h of darkness. All procedures conducted on animals complied with the ARRIVE guidelines and were approved by the Ethics Committee of Southern Medical University.

Mice were randomly divided into seven groups (*n* = 8 per group): a control group; a model group; CDER167 groups with 1, 5 and 10 mg/kg treatment; a RDEA3170 group with 20 mg/kg treatment; and an allopurinol group with 10 mg/kg treatment. To induce hyperuricemia, PO, a uricase inhibitor, was intraperitoneally injected into mice at 300 mg/kg in 0.5% CMC-Na as reported by Wu et al. [22], while the control group was administered 0.5% CMC. One hour after PO injection, the mice received 1, 5 or 10 mg/kg CDER167, 20 mg/kg RDEA3170, or 10 mg/kg allopurinol by oral gavage, according to their grouping. Mice in the control and hyperuricemic groups received vehicle (0.5% CMC). On the 7th day, the mice were fasted for 12 h before drug administration, and

1 h after the last administration, blood samples were obtained from the orbital vein. The samples were then centrifuged (3000  $\times$  *g*, 10 min) to obtain serum and stored at –80 °C for further analysis. Urine samples were collected after drug administration for 12 h in metabolic cages on day 6. The separated serum was obtained by centrifugation at 3000  $\times$  *g* for 10 min and stored at –80 °C. The animals were sacrificed, and the body weights and organ indexes (organ-to-body weight ratios) were recorded. Kidney and liver tissues were removed and weighed after being rinsed with 0.9% saline, and a portion was stored at –80 °C for real-time PCR.

**Sample collection and analysis**

Urine samples were collected after drug administration for 12 h in metabolic cages on day 6. The samples were then centrifuged (3000  $\times$  *g*, 10 min) to obtain the supernatants and stored at –80 °C until analysis. Serum samples were collected 2 h following administration of RDEA3170, CDER167 or allopurinol. The separated serum was obtained by centrifugation at 3000  $\times$  *g* for 10 min and stored at –80 °C. Kidney and liver tissues were removed and weighed after being rinsed with 0.9% saline, and a portion of the tissue was stored at –80 °C for real-time PCR. Body weights and organ indexes (organ-to-body weight ratios) were recorded to assess the safety of CDER167.

**Biochemical parameters**

Serum and urine uric acid as well as serum CR and blood urea nitrogen (BUN) levels were determined by using assay kits according to the manufacturer's instructions.

**RT-qPCR determinations of renal URAT1, GLUT9 and ABCG2 mRNA levels**

Total RNA of kidney tissue was extracted by using an RNA extraction kit (FOREGENE, China). One microgram of RNA was reverse transcribed with SuperScript III reverse transcriptase (Invitrogen, USA) to synthesize 10  $\mu$ L of cDNA template, and the cDNA was diluted fivefold before use in quantitative PCR. PCR amplification was conducted with GAPDH as an external standard. The primers used in this study were as follows (Table 1).

**Western blot**

Western blotting was performed as previously reported [20]. In brief, vesicles (20  $\mu$ g) were subjected to SDS-PAGE (Beyotime Biotechnology, China) and transferred to polyvinylidene fluoride membranes. Membranes were probed with the corresponding primary antibodies against ABCG2 (SAB, CA, USA) and Na<sup>+</sup>-K<sup>+</sup>-ATPase (Proteintech, IL, USA) at 4 °C overnight. The bands were visualized with a gel imaging system. Densitometric analyses were performed by ImageJ software.

**Pharmacokinetics study**

The study protocol was approved by the Ethics Committee of Southern Medical University. Male Sprague–Dawley rats (180  $\pm$  20

**Table 1.** Primers used for RT-qPCR.

Name	Primers
URAT1	Forward: 5'-AGCTCTTGACCCCAATGC-3' Reverse: 5'-CTTCAGAGCGTGAGAGTCACACA-3'
GLUT9	Forward: 5'-TTGCTTTAGCTTCCTGATGTG-3' Reverse: 5'-GAGAGGTTGTACCCGTAGAGG-3'
ABCG2	Forward: 5'-TGCCAGATAAGAGGGGTTAGGT-3' Reverse: 5'-TGCTTCAGTGGAGTTGAGA-3'
$\beta$ -actin	Forward: 5'-AAGTCCCTCACCTCCCAAAAG-3' Reverse: 5'-AAGCAATGCTGCACCTTCCC-3'

g) were provided by the Laboratory Animal Center of Southern Medical University (Guangzhou, China). A total of 16 SD male rats were used in the experiment and divided into four groups according to their average body weight, with 4 rats in each group, to receive intravenous (7.2 mg/kg) or orally administered (7.2 mg/kg) CDER167 or RDEA3170. CDER167 and RDEA3170 were dissolved in 0.5% CMC-Na to prepare a suspension for intragastric administration. For intravenous administration, CDER167 was dissolved in polyethylene glycol 400:water (1:1). Blood samples (0.5 mL) were collected from the orbital vein into heparinized tubes at 0.083, 0.25, 0.5, 0.75, 1, 1.5, 2, 3, 4, 6, 8, 12, 24 and 36 h after oral administration. Similarly, after intravenous administration, blood samples were collected at 0.033, 0.083, 0.25, 0.5, 1, 2, 4, 6, 8, 12, 24 and 36 h. All samples were immediately centrifuged at 8000 r/min for 5 min, and then, the supernatants were stored at  $-80^{\circ}\text{C}$  until analysis. The pharmacokinetic parameters determined included the elimination half-life ( $t_{1/2}$ ), time of peak plasma concentration ( $T_{\text{max}}$ ), maximum plasma concentration ( $C_{\text{max}}$ ), area under the concentration-time curve (AUC), mean residence time (MRT) and bioavailability (F). The relevant pharmacokinetic parameters were calculated using DAS 2.0 software. The obtained plasma samples (100  $\mu\text{L}$ ) were transferred to a clean 1.5 mL centrifuge tube and spiked with 10  $\mu\text{L}$  of the internal standard solution (testosterone, 1  $\mu\text{g}/\text{mL}$ ). The mixture was extracted with 600  $\mu\text{L}$  of ethyl acetate, vortexed for 3 min and centrifuged at 14,000 r/min for 10 min. The supernatant was then transferred to a new 1.5 mL centrifuge tube, 600  $\mu\text{L}$  of ethyl acetate was added to the residue, followed by sonication for 30 s, vortexing for 3 min, and centrifugation at 14,000 r/min for 10 min. Then, the supernatant was combined twice in succession and evaporated to dryness at  $40\text{--}50^{\circ}\text{C}$ . The residue was reconstituted in 400  $\mu\text{L}$  of mobile phase (50% methanol), sonicated for 1 min, vortexed for 3 min, and then centrifuged at 14000 r/min for 15 min. A 300  $\mu\text{L}$  aliquot of the resulting solution was injected into the LC-MS/MS system for analysis.

#### Equipment and analytical conditions

The LC-MS/MS system used was composed of a Shimadzu HPLC system (Shimadzu Nexera LC-30A, Japan) coupled to an API 4000 triple quadrupole mass spectrometer (Applied Biosystems Sciex, Ontario, Canada). Data were processed with SCIEX Analyst software (v. 1.6.3).

Chromatographic separation was performed on a Synergi Fusion-RP C18 column (2 mm  $\times$  50 mm, 4  $\mu\text{m}$ ). The column temperature was set at  $35^{\circ}\text{C}$ . The flow rate was 0.4 mL/min, and the injection volume was 5  $\mu\text{L}$ . For HPLC-MS/MS detection, the mobile phase consisted of water (mobile phase A) and methanol (mobile phase B). In the LC gradient profile, mobile phase B was initially 10% (v/v), linearly increased to 90% from 1.0 to 3.0 min, held at 90% for 2 min, and then returned to 10% from 5.0 to 5.1 min. The chromatographic run time for each sample was 6 min.

Mass spectrometry detection was carried out in positive ion mode using an electrospray ionization (ESI) source. The optimized instrument parameters for monitoring the analytes were as follows: source temperature,  $500^{\circ}\text{C}$ ; ion spray voltage, 5000 V; curtain gas, 15 psi; ion source gas 1, 55 psi; ion source gas 2, 55 psi; dwell time, 120 ms. Quantification was performed in multiple reaction monitoring mode at  $m/z$  363.2/124.2 at 3.10 min for CDER167,  $m/z$  349.2/263.2 at 3.38 min for RDEA3170 and  $m/z$  289.2/109.2 at 3.43 min for the IS (testosterone).

Validation of this method, including the selectivity, linearity, lower limit of quantification, accuracy, precision, extraction recovery, matrix effects, and stability, is presented in the Supplementary materials (Fig. S2 and Tables S1–S3).

#### Metabolic stability

CDER167 and RDEA3170 (3 and 0.3  $\mu\text{M}$ ) were incubated with human liver microsomes (0.4 mg protein/mL) in a final volume of

500  $\mu\text{L}$ . The mixture contained NADPH (1.3 mM NADP, 3.3 mM glucose 6-phosphate and 0.4 U/mL glucose 6-phosphate dehydrogenase), magnesium chloride (3 mM), and potassium phosphate buffer (100 mM, pH 7.4). The experiment was performed in duplicate, and zero-time incubations served as negative controls. The reaction was initiated by the addition of HLMs (0.4 mg protein/mL) followed by incubation for 15, 30, or 60 min at  $37^{\circ}\text{C}$ . The reaction was terminated by the addition of 1 mL of methanol.

#### Evaluation on hERG $\text{K}^{+}$ channel inhibition

Wild-type Chinese hamster ovary cells transiently transfected with hERG potassium channels (CHO-K1/hERG) were maintained in culture medium. Cells were cultured for 24 h and then used for electrophysiological recordings. Voltage-clamp recording was performed in the whole-cell patch-clamp configuration.

The extracellular solution consisted of 140 mM NaCl, 5 mM KCl, 1 mM  $\text{MgCl}_2$ , 2 mM  $\text{CaCl}_2$ , 10 mM HEPES, and 10 mM D-glucose. After preparation, NaOH was used to adjust the pH to  $\sim 7.4$ . The intracellular solution consisted of 140 mM KCl, 1 mM  $\text{MgCl}_2$ , 5 mM EGTA, and 10 mM HEPES. Cisapride, CDER167, and RDEA3170 were dissolved in DMSO to obtain working solutions with the extracellular solution. The electrophysiology recording of hERG channel current was carried out following a protocol described previously [23]. Whole-cell recordings were analyzed using Clampfit 10.6 software. Figures were plotted using GraphPad Prism 8.0. All experiments were performed in duplicate for  $\text{IC}_{50}$  determination. Cisapride was used as a positive control [24, 25].

#### Exploration of potential CDER167 binding sites in URAT1

S35, F365 and I481 were previously reported by Tan PK [26] to be RDEA3170 binding sites in URAT1. Consistent with this study, several mutants (S35N, F365Y and I481A) were constructed to explore the difference in URAT1 inhibition between CDER167 and RDEA3170. Specific mutants were generated by site-directed mutagenesis using a Transgene Mutagenesis Kit (Beijing, China); the primers used in this procedure are shown in Table 2. Mutations were further confirmed with a DNA sequencing analyzer (Applied Biosystems, Foster City, CA, USA). HEK293 cells were transiently transfected with the mutants as described above. The inhibitory effects of CDER167 on URAT1-S35N, URAT1-F365Y and URAT1-I481A were determined and compared with its effects on URAT1-WT.

#### Statistical analysis

Data were calculated as the mean  $\pm$  Standard Deviation and analyzed with a  $t$ -test or one-way ANOVA using GraphPad (La Jolla, CA, USA). A value of  $P < 0.05$  was considered statistically significant.

## RESULTS

CDER167 inhibits the urate transport activity of URAT1 in vitro. To verify the reliability of the experimental system, the inhibitory effects of two other reported URAT1 inhibitors, benzbramarone [9, 27] and probenecid [28], were determined. As shown in Fig. 1, the inhibitory effect of CDER167 on URAT1 was similar to that of

**Table 2.** Primers used for mutagenesis.

Mutation	Primers
S35N	Forward:5'-TGTGTACCCAGAATATGCTGGAG-3' Reverse:5'-CTCCAGCATATTCTGGGTACACA-3'
F365Y	Forward:5'-GGCTTCACCTTCTACGGCTGGC-3' Reverse:5'-GCCAGGCCGTAGAAGGTGAAGCC-3'
I481A	Forward:5'-TGGAGGAGCCGCACTGGGGCC-3' Reverse:5'-GGCCCCAGTGCGGCTCTCCA-3'

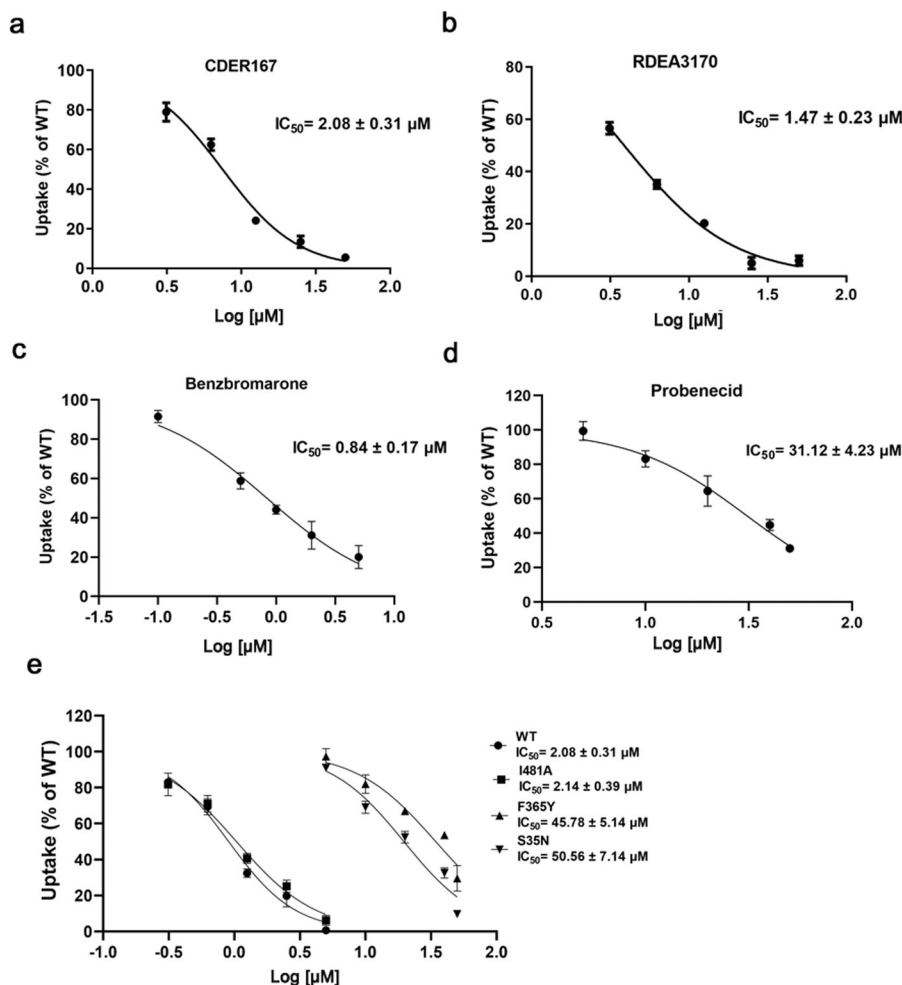


**Fig. 1** CDER167 inhibits URAT1 in vitro. **a–d** Dose-dependent effects of CDER167, RDEA3170, benzbromarone and probenecid on the uptake of [ $^{14}$ C]-uric acid by HEK293 cells expressing URAT1.  $n = 6$ . **e** Potential binding residues of CDER167 with URAT1 determined by a combination of site-directed mutagenesis and [ $^{14}$ C]-uric acid uptake assays. The data are expressed as the mean  $\pm$  SD.

RDEA3170, with  $IC_{50}$  values of  $2.08 \pm 0.31 \mu\text{M}$  and  $1.47 \pm 0.23 \mu\text{M}$ , respectively, which were both weaker than that of benzbromarone ( $IC_{50} = 0.84 \pm 0.17 \mu\text{M}$ ) but significantly stronger than that of probenecid ( $IC_{50} = 31.12 \pm 4.23 \mu\text{M}$ ).

Previous studies have reported that RDEA3170 has high potency against URAT1, and residues S35, F365 and I481 [29] located in TMDs 1, 7 and 11, respectively, all contribute to RDEA3170 affinity. To investigate the binding sites of CDER167 and subtle differences between its activity and that of RDEA3170, the mutants URAT1-S35N, URAT1-F365Y and URAT1-I481A were established by site-directed mutagenesis, and the  $IC_{50}$  values were determined. The results showed that the inhibitory effects of CDER167 on URAT1 was significantly reduced when S35 and F365 were mutated (Fig. 1e). The  $IC_{50}$  values increased significantly (20–25-fold) when S35 and F365 were mutated, indicating that S35 and F365 might be in the active site of CDER167 binding. Interestingly, when I481 was mutated to alanine, the uptake activity of URAT1 was not affected, indicating that I481 does not contribute to CDER167 affinity, which may explain why the activity of CDER167 is slightly weaker than that of RDEA3170 against URAT1 in vitro.

CDER167 inhibits the urate transport activity of GLUT9 in vitro. RDEA3170 has been reported to be a URAT1 inhibitor. We next aimed to investigate whether RDEA3170 and CDER167 affect GLUT9. Interestingly, RDEA3170 had no effect on the current

generated by GLUT9, while CDER167 showed enhanced inhibition of GLUT9 (Fig. 2a) at  $100 \mu\text{M}$ .

We further explored the GLUT9 inhibitory activity of CDER167 using benzbromarone and probenecid as positive controls. We found that CDER167 inhibited GLUT9 in an irreversible manner. The  $IC_{50}$  of CDER167 was calculated to be  $91.55 \pm 15.28 \mu\text{M}$ , which is weaker than that of benzbromarone ( $IC_{50} = 31.45 \pm 10.45 \mu\text{M}$ ) but significantly more potent than probenecid ( $IC_{50} = 636.30 \pm 10.40 \mu\text{M}$ ) (Fig. 2b). However, lesinurad and allopurinol showed no inhibitory effects on GLUT9, as reported by our previous study. As indicated in Fig. 2c, the inhibitory effect of CDER167 on GLUT9 was still present when drug perfusion was removed, which is consistent with the phenomenon observed with benzbromarone.

CDER167 has minimal effects on ABCG2 in vitro compared with RDEA3170

Inhibition of urate secretion transporters has been reported to aggravate the burden of hyperuricemia [30]. ABCG2 is a physiologically important urate secretion exporter. In the present study, we examined the transport of uric acid via ABCG2. First, HEK293 cells were induced to express ABCG2, and plasma membrane vesicles were prepared. ABCG2 expression in the prepared vesicles was detected by Western blotting (Fig. 3a). To examine the urate transport activity of ABCG2, membrane vesicles were incubated with  $25 \mu\text{M}$  [ $^{14}$ C]-uric acid in the presence or absence of ATP. Compared with the mock vesicles, the ABCG2-expressing HEK293 membrane

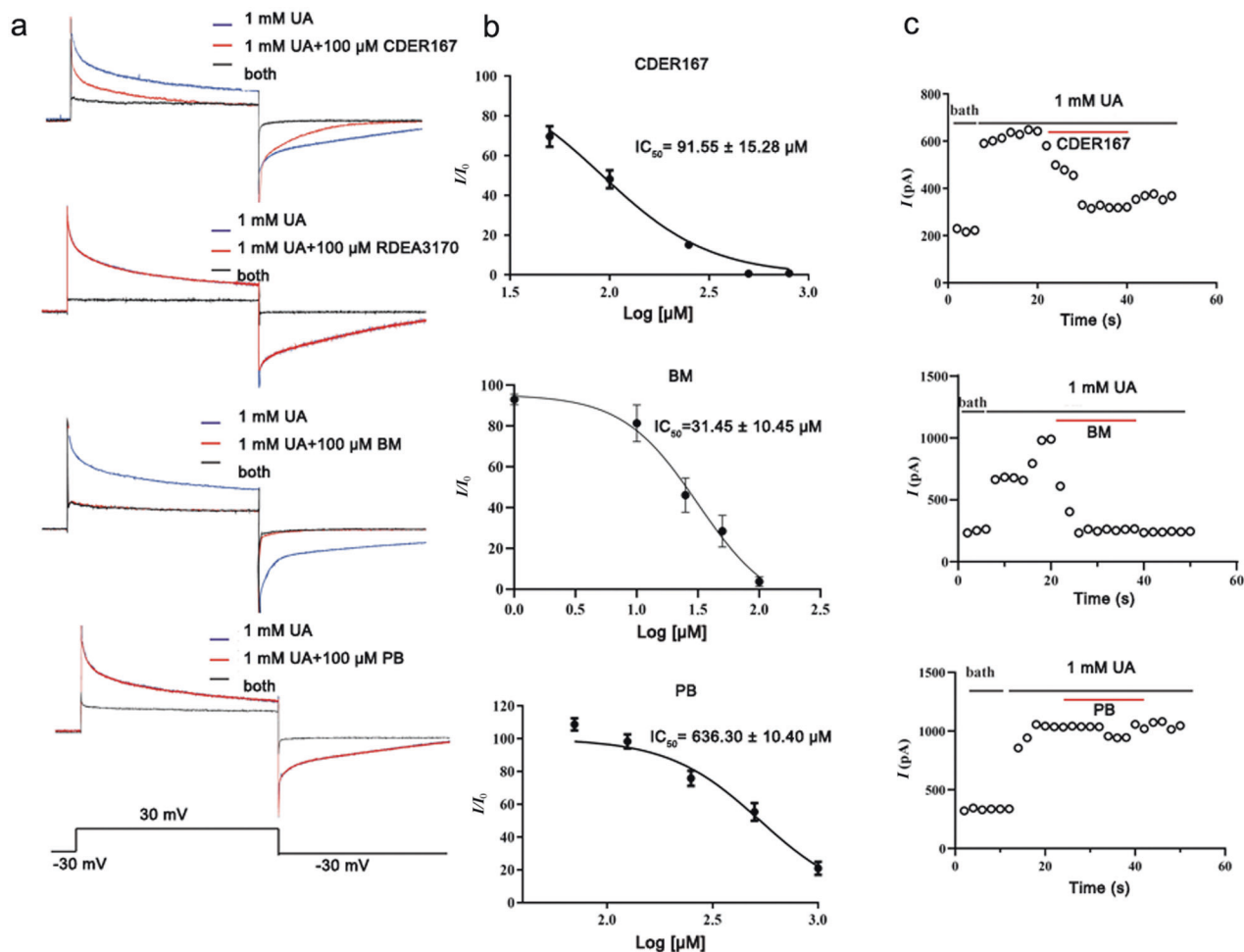


**Fig. 2** CDER167 inhibits GLUT9 in vitro. **a** Original current traces of GLUT9-expressing HEK293T cells induced by 1 mM uric acid (UA) in the presence (red) or absence (green) of 100  $\mu\text{M}$  CDER167, RDEA3170, benzbromarone and probenecid. **b** Dose-response relationship of GLUT9 currents by CDER167, benzbromarone and probenecid. **c** Time course of current with the perfusion of CDER167 (100  $\mu\text{M}$ ), benzbromarone (100  $\mu\text{M}$ ) or probenecid (100  $\mu\text{M}$ ) after stimulation with 1 mM UA.  $n = 6$ . The data are expressed as the mean  $\pm$  SD of at least three independent experiments.

vesicles (ABCG2 vesicles) showed better uric acid transport ability (Fig. 3b), indicating that the prepared ABCG2 vesicles had the ability to transport uric acid and were capable of being used in subsequent experiments.

The experimental results showed that RDEA3170 inhibited ABCG2 with an  $IC_{50}$  value of  $16.39 \pm 2.15 \mu\text{M}$ , while CDER167 inhibited ABCG2 with an  $IC_{50}$  of  $144.23 \pm 6.78 \mu\text{M}$ , which is ninefold weaker than that of RDEA3170 (Fig. 3c). Benzbromarone was used as a positive control ( $IC_{50} = 1.08 \pm 0.36 \mu\text{M}$ ), which showed a result similar to reported data [31].

#### Effectiveness and safety of CDER167 in hyperuricemic mice

PO injection significantly increased the serum uric acid levels compared to the normal control group, as presented in Fig. 4a. Allopurinol, a xanthine oxidase inhibitor acting as a positive control, notably decreased the serum uric acid level, indicating that this model was suitable for the evaluation of antihyperuricemic agents. Notably, CDER167 at 10 mg/kg was able to significantly decrease the serum uric acid level and increase the urine uric acid level (Fig. 4a, b). However, the antihyperuricemic effect of RDEA3170 at 20 mg/kg was slightly weaker than that of CDER167 at 10 mg/kg, with mean values of  $360.06 \mu\text{M}$  and  $341.08 \mu\text{M}$ , respectively. In addition, the uricosuric effect of RDEA3170 was almost undetectable (Fig. 4b), which was notably different from

that of CDER167 at 5 mg/kg and 10 mg/kg. CDER167 at 10 mg/kg significantly increased the urine uric acid level from  $476.39 \mu\text{M}$  to  $809.83 \mu\text{M}$  compared with the model group. As shown in Fig. 4c, d, administration of CDER167 for 7 days showed no effect on the serum CR and BUN levels, suggesting its safety in the kidney. Moreover, the data in Fig. S3 show that CDER167 had no effect on body weight or liver/kidney indexes. All these data proved that the application of a certain dose of CDER167 is safe for mice with hyperuricemia and can effectively reduce serum uric acid levels.

#### Effects of CDER167 on URAT1, GLUT9 and ABCG2 mRNA expression in kidneys

Many urate-lowering agents have been reported to affect the expression of urate transporters in vivo [32, 33]. Therefore, we detected the relative transporter expression levels in the kidney. We observed that the mRNA expression levels of URAT1 and GLUT9 were significantly upregulated in the model group. CDER167 significantly decreased URAT1 and GLUT9 expression at doses between 5 and 10 mg/kg (Fig. 5a, b). In contrast to URAT1 and GLUT9, the results showed that CDER167, RDEA3170 and AP upregulated the mRNA expression of ABCG2 compared with the model group in the kidney, the expression of ABCG2 was lower than that in the control group, and treatment with CDER167 increased the expression of ABCG2 (Fig. 5c).

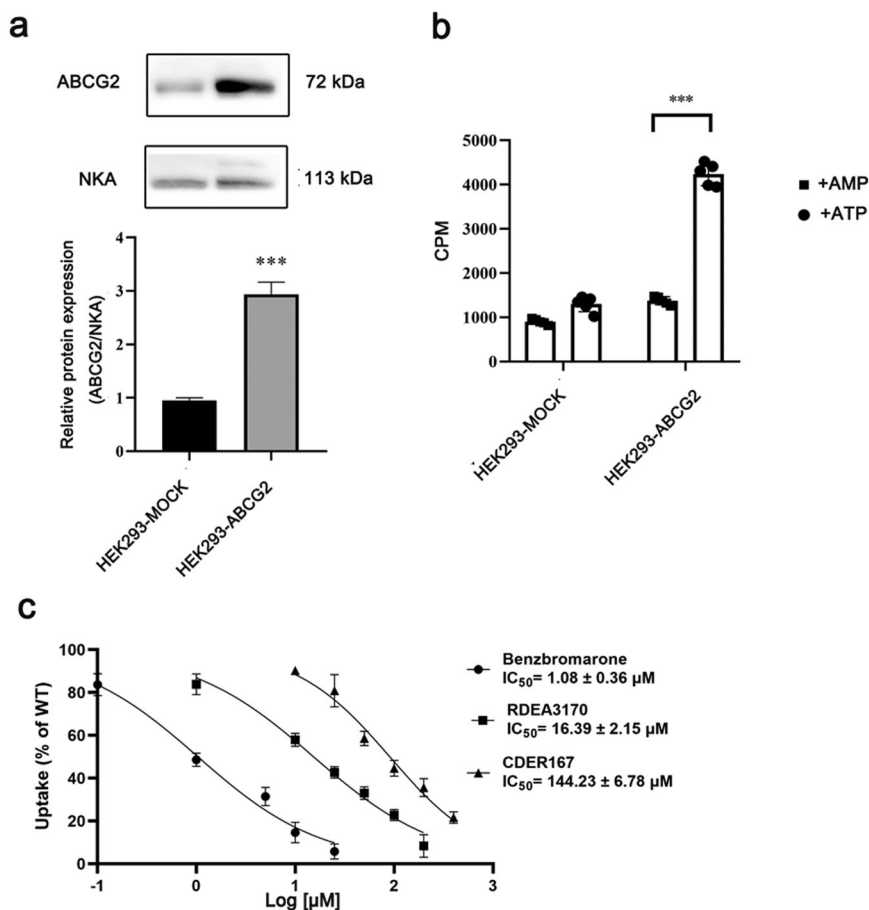


**Fig. 3** CDER167 inhibits ABCG2 in vitro. **a** Membrane protein expression levels of HEK293-MOCK and HEK293-ABCG2 cells.  $n = 3$ . **b** [ $^{14}\text{C}$ ]-Uric acid transport of vesicles with or without ATP.  $n = 5$ . **c** Dose-dependent effects of CDER167, RDEA3170 and benzbromarone on the uptake of [ $^{14}\text{C}$ ]-uric acid by HEK293-ABCG2 vesicles.  $n = 3$ . The data are expressed as the mean  $\pm$  SD of at least three independent experiments.  $***P < 0.001$  compared with the corresponding group.

To investigate whether these compounds could directly affect the mRNA expression of URAT1, GLUT9 and ABCG2, mouse renal tubular epithelial (mTEC) cells were incubated with 100  $\mu\text{M}$  CDER167, RDEA3170 and AP for 2 h as previously reported [33]. The data showed that the mRNA expression of transporters was not affected by CDER167, RDEA3170 or AP treatment (Fig. 5d), suggesting that they might have no direct effects on the expression of these transporters.

#### Pharmacokinetic study

To study the pharmacokinetic characteristics of CDER167, we measured the plasma concentration of CDER167 after i.v. or p.o. administration to rats, with RDEA3170 as a control. The pharmacokinetic parameters were calculated and are summarized in Fig. 6 and Table 3. As shown in Fig. 6a, the mean plasma concentration-time curves for the CDER167 and RDEA3170 groups were similar after i.v. administration. Parameters, such as the MRT,  $t_{1/2}$  and AUC, were analogous between CDER167 and RDEA3170 after i.v. treatment, but the  $t_{1/2}$  of CDER167 was shorter than that of RDEA3170 after oral administration. In this study, the  $C_{\text{max}}$  of CDER167 was slightly higher and occurred earlier than that of RDEA3170 after both i.v. and p.o. administration (Fig. 6a, b). Furthermore, the calculated oral bioavailability of CDER167 was higher than that of RDEA3170, with values of  $27.17\% \pm 1.80\%$  and  $20.92\% \pm 7.65\%$ , respectively. These data might help explain why the uric acid-lowering effect of CDER167 is better in vivo within 2 h after administration.

#### Metabolic stability

CDER167 and RDEA3170 were coincubated with human liver microsomes to evaluate their metabolic stability. As shown in Fig. 7, the metabolic rate for 3 or 0.3  $\mu\text{M}$  CDER167 was slower than that for RDEA3170 under the same conditions, especially within 20–30 min, indicating that RDEA3170 was less stable in human liver microsomes than CDER167.

#### Assessment of hERG inhibition activity

Compounds with high affinity for hERG potassium channels may show severe cardiotoxicity due to the induction of prolonged QT intervals. Therefore, we tested the hERG inhibition activity of CDER167 in vitro using a manual patch-clamp method. As shown in Fig. 8, neither CDER167 nor RDEA3170 inhibited the potassium channel at 100  $\mu\text{M}$ , while the positive drug cisapride at a concentration of 1  $\mu\text{M}$  led to a 50% reduction in the potassium channel, which was consistent with a previous study [25].

#### DISCUSSION

The prevalence of hyperuricemia is increasing yearly with changes in diet structure and the extension of life expectancy [34–36]. The objective of hyperuricemia treatment is to effectively reduce the serum uric acid level [37]. Studies have shown that ~90% of primary hyperuricemia is related to uric acid excretion disorder, and thus, promoting uric acid excretion is the key to preventing and controlling hyperuricemia. URAT1 and GLUT9 [38, 39] are

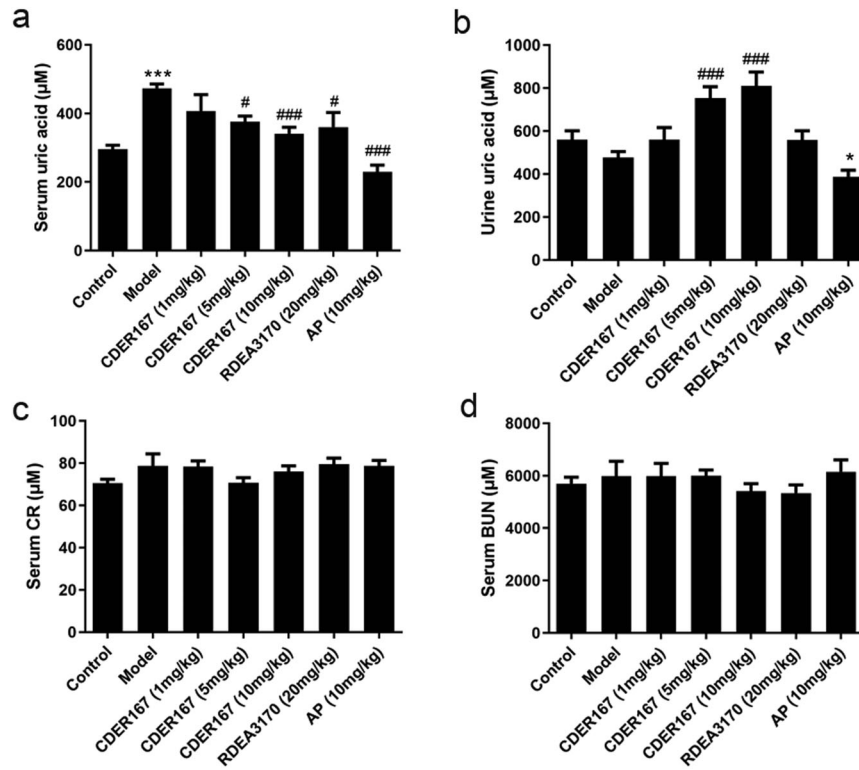


**Fig. 4 CDER167 reduces serum uric acid in vivo.** Effects of CDER167 on (a) serum uric acid, (b) urine uric acid, and serum (c) CR and (d) BUN levels in hyperuricemic mice.  $n = 8$ . The data are expressed as the mean  $\pm$  SD. \*\*\* $P < 0.001$  compared with the control group; # $P < 0.05$  and ### $P < 0.001$  compared with the model group.

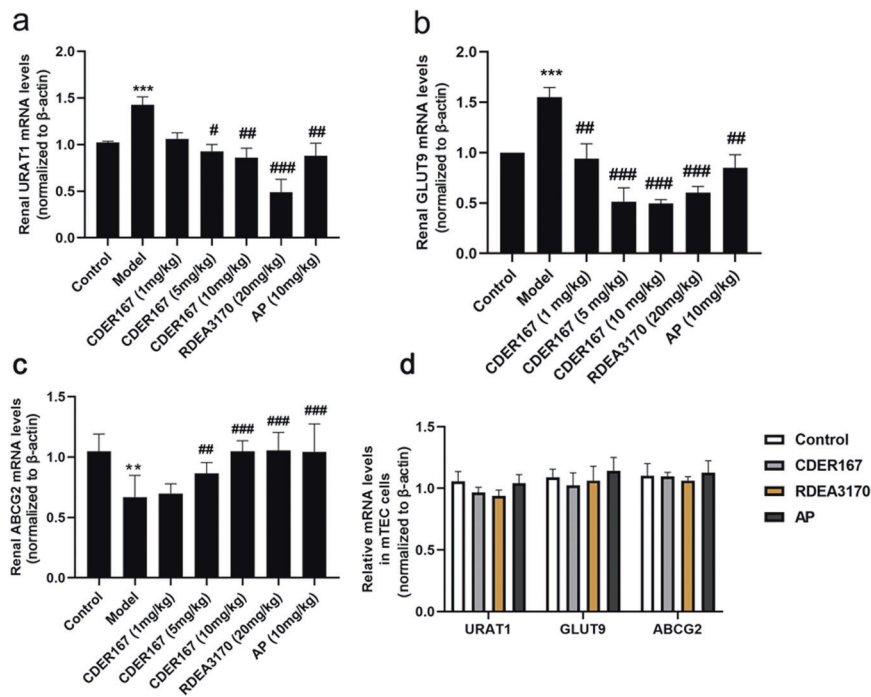


**Fig. 5 CDER167 regulates mRNA expression of URAT1, GLUT9 and ABCG2 in kidney.** Effects of CDER167 on renal (a) URAT1, (b) GLUT9 and (c) ABCG2 mRNA expression levels in vivo.  $n = 6$ . The data are expressed as the mean  $\pm$  SD. **d** Relative mRNA expression levels of URAT1, GLUT9 and ABCG2 in mTECs incubated with 100 μM CDER167, RDEA3170 or AP for 2 h. \* $P < 0.05$  and \*\*\* $P < 0.001$  compared with the control group; # $P < 0.05$ , ## $P < 0.01$ , ### $P < 0.001$  compared with the model group.



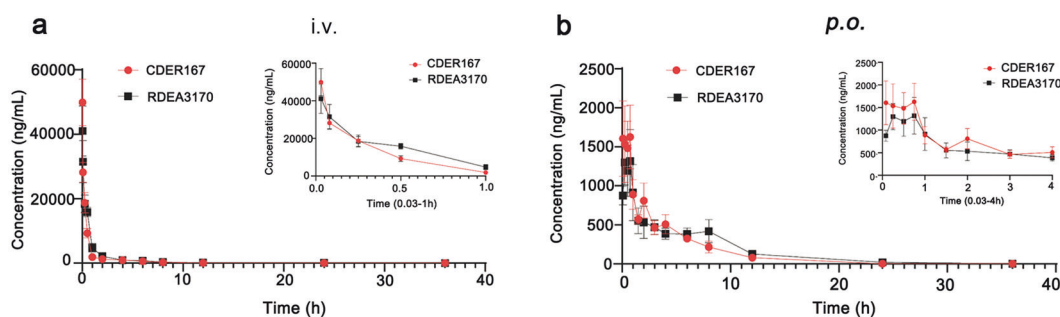


**Fig. 6** Mean plasma concentration-time profiles. **a** CDER167 and RDEA3170 after i.v. administration at 7.2 mg/kg (mean  $\pm$  SD,  $n = 4$ ). **b** CDER167 and RDEA3170 after *p.o.* administration at 7.2 mg/kg (mean  $\pm$  SD,  $n = 4$ ).

**Table 3.** The main pharmacokinetic parameter of RDEA3170 and CDER167 after administration (mean  $\pm$  SD,  $n = 4$ ).

PK parameter	<i>p.o.</i>		i.v.	
	RDEA3170	CDER167	RDEA3170	CDER167
$T_{max}$ (h)	0.50 $\pm$ 0.25	0.46 $\pm$ 0.29	0.04 $\pm$ 0.02	0.03 $\pm$ 0.00
$C_{max}$ (ng/mL)	1433.46 $\pm$ 455.22	1864.47 $\pm$ 599.80	46189.88 $\pm$ 7704.40	49896.57 $\pm$ 10704.49
$t_{1/2}$ (h)	4.14 $\pm$ 1.19	3.12 $\pm$ 1.36	3.40 $\pm$ 1.49	2.41 $\pm$ 0.53
AUC <sub>(0-∞)</sub> (ng/mL*h)	6320.59 $\pm$ 2311.73	5632.57 $\pm$ 372.95	30214.66 $\pm$ 4369.80	20728.37 $\pm$ 3565.70
MRT <sub>(0-∞)</sub> (h)	6.23 $\pm$ 0.41	5.15 $\pm$ 1.01	2.16 $\pm$ 0.51	1.96 $\pm$ 0.28
$F$ (%)	20.92 $\pm$ 7.65	27.17 $\pm$ 1.80		

closely related to uric acid homeostasis and cooperate to complete the process of uric acid reabsorption; thus, in recent years, they have become important targets for the development of uric acid-lowering drugs.

Currently, urate excretion-promoting drugs used in the clinic primarily act on URAT1 and increase uric acid excretion by inhibiting uric acid reabsorption in the proximal renal tubules. Benzbromarone and probenecid inhibit not only URAT1 but also OAT1 and ABCG2. Inhibition of OAT1 and ABCG2 might partially cancel urate-lowering effects of these compounds. In the present study, we observed that they also inhibited GLUT9 (Fig. 2). In addition, all of these compounds have severe drawbacks, such as the idiosyncratic hepatotoxic adverse effects of benzbromarone [40] and the poor efficacy of probenecid [41]. Selective urate reabsorption inhibitors are expected to be a new trend for the treatment of hyperuricemia. Lesinurad modestly inhibited URAT1 in vitro and has been recommended for use at 200 mg [10] daily, but renal toxicity limits its clinical use [42]. RDEA3170, a lesinurad analog, is a selective and effective URAT1 inhibitor that has been developed to treat patients with gout or asymptomatic hyperuricemia [26, 43, 44]. Lesinurad and RDEA3170 are novel selective URAT1 inhibitors without GLUT9 inhibition at 100  $\mu$ M. However, CDER167, an analog of RDEA3170, showed dual inhibitory effects on both URAT1 and GLUT9, which is the unique dual-target inhibitory activity of this type of compound. In addition, we further explored the effects of CDER167 on ABCG2, and the results showed no obvious effects from CDER167 at 100  $\mu$ M on the ABCG2 transporter.

URAT1 and GLUT9 belong to the major facilitator superfamily (MFS) [45] and have a pivotal role in urate reabsorption in the kidneys. They share similar membrane topology and a similar structural characteristic fold, known as the MFS fold [46]. These transporters undergo a series of conformational changes, including an outward-open conformation, occluded state and inward-open conformation, to perform substrate translocation [47]. A transport tunnel is located in the central region and is composed of multiple transmembrane domains; thus, we believe that

inhibitors with a flexible linker could twist and bind better to transporters.

In this study, based on the "flexible theory" we proposed, a methylene unit was introduced between the naphthalene and pyridine moieties in RDEA3170, and this new molecule was named CDER167. We found that CDER167 inhibited both URAT1 and GLUT9 in vitro and in vivo and played a significant role in uric acid excretion. Moreover, the in vitro URAT1 inhibitory activity of CDER167 was similar to that of RDEA3170. To explore the slight differences in the activities of the two molecules, we investigated the potential binding residues of CDER167 in URAT1 compared with those of RDEA3170. The results showed that CDER167 shared the same binding residues (S35 and F365) with RDEA3170 except for I481, which might help explain the slight difference in URAT1 inhibitory potency in vitro. The increased flexibility of CDER167 makes it more susceptible to structural transformation, enabling it to simultaneously inhibit GLUT9 in a dose-dependent manner, while RDEA3170 showed no effect on GLUT9 transport at concentrations  $>100$   $\mu$ M. Further experiments revealed that the inhibitory effects of CDER167 on GLUT9 continued after CDER167 was removed from the extracellular fluid, indicating that the inhibitory effect of CDER167 on GLUT9 is irreversible, similar to the effect of benzbromarone. Inhibition of ABCG2 has been reported to neutralize uricosuric effects. RDEA3170 also inhibited the urate secretion transporter ABCG2, but CDER167 showed ninefold weaker inhibition than RDEA3170, which suggests that CDER167 is a more selective urate reabsorption transporter inhibitor than RDEA3170.

In the in vivo study, CDER167 significantly promoted the excretion of excess serum uric acid in the urine and reduced the serum uric acid levels in PO-induced hyperuricemic mice in a dose-dependent manner. The PO-induced model is widely used for pharmacological evaluation of urate-lowering drugs [48]. In the present study, we mainly aimed to compare the effects of CDER167 and RDEA3170 in reducing uric acid levels. Therefore, we chose RDEA3170 and allopurinol as positive controls. Allopurinol always shows strong urate-lowering effects in the hyperuricemia mouse

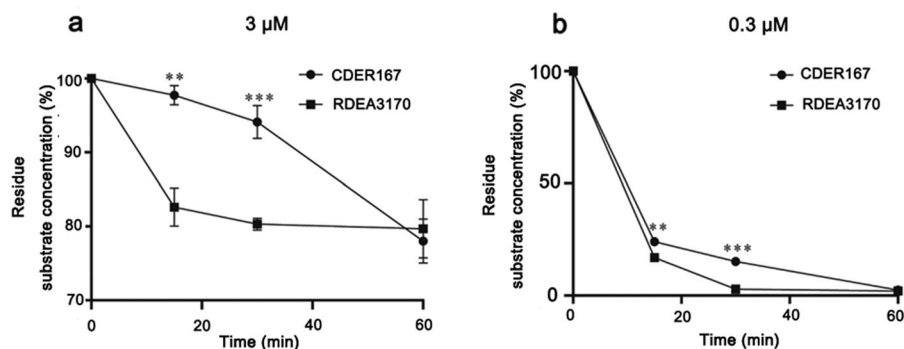


**Fig. 7 Metabolic stability.** Metabolic stability of (a) 3  $\mu\text{M}$  CDER167 and (b) 0.3  $\mu\text{M}$  CDER167 in human liver microsomes compared to RDEA3170. The results are expressed as the % of remaining substrate concentration ratio of each compound after different incubation times. The data are shown as the mean  $\pm$  SD.  $n = 4$ .  $**P < 0.01$ ,  $***P < 0.001$  compared with the RDEA3170 group.

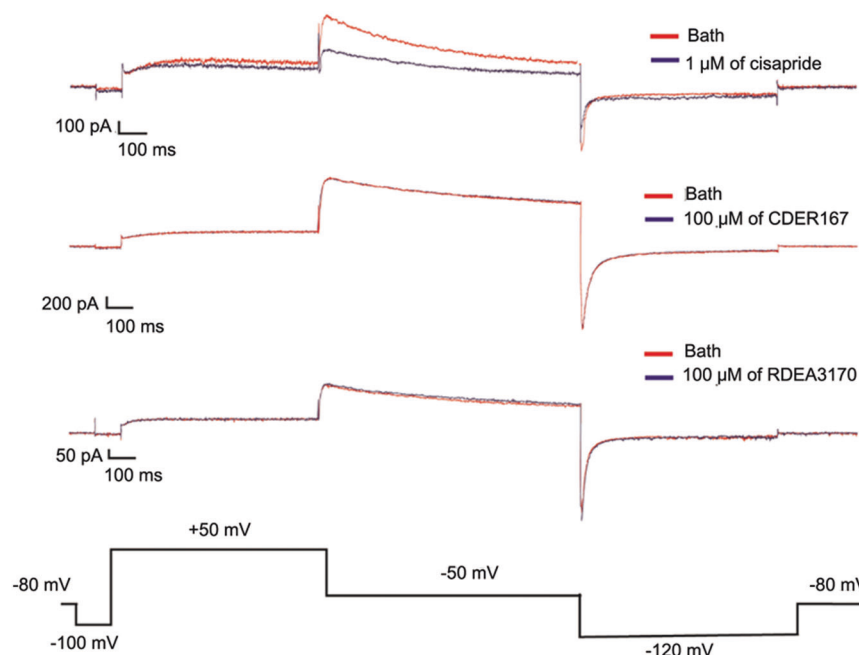


**Fig. 8 hERG toxicity of CDER167 and RDEA3170.** The figures shown above are the original current traces of CHO-K1 cells expressing hERG potassium channels in the presence (purple) or absence (red) of 1  $\mu\text{M}$  cisapride, 100  $\mu\text{M}$  CDER167 and 100  $\mu\text{M}$  RDEA3170. Cisapride (1  $\mu\text{M}$ ) was used as a positive control.

model [49], so we could know whether the system was reliable. Serum uric acid was close to 500  $\mu\text{M}$  in the model group, a 1.5-fold increase compared to the control group (300  $\mu\text{M}$ ), which is similar to reported data [50]. Surprisingly, CDER167 showed better uric acid-lowering activity at lower dosages (10  $\text{mg}\cdot\text{kg}^{-1}\cdot\text{d}^{-1}$ ) than RDEA3170 (20  $\text{mg}/\text{kg}$ ). CDER167 showed better serum urate-lowering effects than RDEA3170 *in vivo*, even though it displayed weaker inhibitory activity on URAT1 than RDEA3170 *in vitro*. One possible reason might be the inhibition of both URAT1 and GLUT9 by CDER167, whereas RDEA3170 inhibits only URAT1. Another reason might be that RDEA3170 showed stronger ABCG2 inhibitory activity than CDER167 so that the urate-lowering effects were partially cancelled. In brief, CDER167 was more effective than RDEA3170 *in vivo*.

Previous studies have widely shown that almost all urate-lowering agents are able to alter the expression of urate transporters *in vivo*. To clarify whether these agents have direct effects on the expression of these transporters, we incubated CDER167, RDEA3170, and allopurinol in mTEC cells for 2 h and observed that they did not change the mRNA expression levels of related transporters *in vitro*. Therefore, we believe that this is a

compensatory regulation process of the body due to changes in uric acid levels but not the direct effect of these agents on the expression of urate transporters. The possible mechanism for the altered expression of these transporters might be due to changes in signaling pathways, such as TLR4-NLRP3, PI3K/Akt [51] and PDZK1 [52, 53], which might be influenced by uric acid stimulation. However, further studies need to be conducted to reveal how uric acid regulates the expression of urate transporters.

The pharmacokinetic studies showed that the  $C_{\text{max}}$  of CDER167 was higher than that of RDEA3170 and that the  $T_{\text{max}}$  was shorter than that of RDEA3170. In addition, the bioavailability of CDER167 was significantly better than that of RDEA3170, and the stability of CDER167 in human liver microsomes was better than that of RDEA3170. These results may explain why CDER167 showed better uric acid-lowering activity than RDEA3170 in hyperuricemic mice.

In addition to the kidneys, the intestine is also an important organ for uric acid excretion. One-third of uric acid in the body is excreted through the intestine [54, 55]. A growing number of studies have suggested that uric acid excretion disorder in the intestine is important in the pathogenesis of primary hyperuricemia [56, 57]. The known intestinal urate transporters are GLUT9

[58] and ABCG2 [59]. Mice with intestine-specific GLUT9 gene knockout showed a significant increase in blood uric acid accompanied by metabolic syndrome [60]. However, the mechanism by which GLUT9 transports uric acid from the intestinal epithelium to the epithelium is not clear. Interestingly, in our previous study, we detected URAT1 and GLUT9 expression in the colon tissue of hyperuricemic mice and found that the URAT1 and GLUT9 mRNA expression levels in the colon tissue of hyperuricemic mice were significantly increased. Moreover, the fold increase of URAT1 was larger than that of GLUT9 (Supplementary Fig. S4), suggesting that URAT1 in the colon may also be involved in intestinal uric acid excretion. We speculate that the uric acid-lowering effects of CDER167 may be related to its simultaneous inhibition of URAT1 and GLUT9 in the intestine, which needs further investigation.

## CONCLUSION

In summary, this study reported that a urate-lowering compound, CDER167, showed similar dual-target inhibition of URAT1 and GLUT9. CDER167 showed minimal ABCG2 inhibitory activity compared with its lead compound RDEA3170 and had more potent uric acid-lowering activity *in vivo*. From the perspective of safety, animal experiments and an assessment of hERG inhibition activity fully proved the safety of CDER167. In addition, the bioavailability of CDER167 is significantly better than that of RDEA3170. We present CDER167 as a promising uricosuric candidate worthy of further development.

## ACKNOWLEDGEMENTS

This work was supported by the National Natural Science Foundation of China (81773794 and 81974507) and the Natural Science Foundation of Guangdong Province (2018A0303130088).

## AUTHOR CONTRIBUTIONS

JXP, YXT and JYG conceived and designed the research. ZAZ, YJ, YYC and QSL conducted the experiments. LL, YML YC and CTL analyzed the results. TW, YY and PZZ wrote the paper. All authors read and approved the paper.

## ADDITIONAL INFORMATION

**Supplementary information** The online version contains supplementary material available at <https://doi.org/10.1038/s41401-021-00640-5>.

**Competing interests:** The authors declare no competing interests.

## REFERENCES

- Dalbeth N, Merriman TR, Stamp LK. Gout. *Lancet*. 2016;388:2039–52.
- Dalbeth N, Phipps-Green A, House ME, Gamble GD, Horne A, Stamp LK, et al. Body mass index modulates the relationship of sugar-sweetened beverage intake with serum urate concentrations and gout. *Arthritis Res Ther*. 2015;17:263.
- Wu J, Zhang YP, Qu Y, Jie LG, Deng JX, Yu QH. Efficacy of uric acid-lowering therapy on hypercholesterolemia and hypertriglyceridemia in gouty patients. *Int J Rheum Dis*. 2019;22:1445–51.
- Hou YL, Yang XL, Wang CX, Zhi LX, Yang MJ, You CG. Hypertriglyceridemia and hyperuricemia: a retrospective study of urban residents. *Lipids Health Dis*. 2019;18:81.
- Wang Y, Chi J, Che K, Chen Y, Sun X, Wang Y, et al. Fasting plasma glucose and serum uric acid levels in a general Chinese population with normal glucose tolerance: a U-shaped curve. *PLoS ONE*. 2017;12:e180111.
- Huffman JE, Albrecht E, Teumer A, Mangino M, Kapur K, Johnson T, et al. Modulation of genetic associations with serum urate levels by body-mass-index in humans. *PLoS ONE*. 2015;10:e119752.
- Kanbay M, Jensen T, Solak Y, Le M, Roncal-Jimenez C, Rivard C, et al. Uric acid in metabolic syndrome: from an innocent bystander to a central player. *Eur J Intern Med*. 2016;29:3–8.
- So A, Thorens B. Uric acid transport and disease. *J Clin Invest*. 2010;120:1791–9.
- Strilchuk L, Fogacci F, Cicero AF. Safety and tolerability of available urate-lowering drugs: a critical review. *Expert Opin Drug Saf*. 2019;18:261–71.
- Miner JN, Tan PK, Hyndman D, Liu S, Iverson C, Nanavati P, et al. Lesinurad, a novel, oral compound for gout, acts to decrease serum uric acid through inhibition of urate transporters in the kidney. *Arthritis Res Ther*. 2016;18:214.
- Hautekeete ML, Henrion J, Naegels S, DeNeve A, Adler M, Deprez C, et al. Severe hepatotoxicity related to benzarone: a report of three cases with two fatalities. *Liver*. 1995;15:25–9.
- Gutman J, Kachur SP, Slutsker L, Nzila A, Mutabingwa T. Combination of probenecid-sulphadoxine-pyrimethamine for intermittent preventive treatment in pregnancy. *Malar J*. 2012;11:39.
- Robinson PC, Dalbeth N. Lesinurad for the treatment of hyperuricaemia in people with gout. *Expert Opin Pharmacother*. 2017;18:1875–81.
- Shen Z, Gillen M, Miner JN, Bucci G, Wilson DM, Hall JW. Pharmacokinetics, pharmacodynamics, and tolerability of verinurad, a selective uric acid reabsorption inhibitor, in healthy adult male subjects. *Drug Des Devel Ther*. 2017;11:2077–86.
- Wu T, Chen J, Dong S, Li H, Cao Y, Tian Y, et al. Identification and characterization of a potent and selective inhibitor of human urate transporter 1. *Pharmacol Rep*. 2017;69:1103–12.
- Bibert S, Hess SK, Firsov D, Thorens B, Geering K, Horisberger JD, et al. Mouse GLUT9: evidences for a urate uniporter. *Am J Physiol Ren Physiol*. 2009;297:F612–9.
- Tian H, Liu W, Zhou Z, Shang Q, Liu Y, Xie Y, et al. Discovery of a flexible triazolylbutanoic acid as a highly potent uric acid transporter 1 (URAT1) inhibitor. *Molecules*. 2016;21:1543.
- Zhao T, Zhao Z, Lu F, Chang S, Zhang J, Pang J, et al. Two- and three-dimensional QSAR studies on hURAT1 inhibitors with flexible linkers: topomer CoMFA and HQSAR. *Mol Divers*. 2020;24:141–54.
- Chen Y, Zhao Z, Li Y, Yang Y, Li L, Jiang Y, et al. Baicalein alleviates hyperuricemia by promoting uric acid excretion and inhibiting xanthine oxidase. *Phytomedicine*. 2020;80:153374.
- Chen Y, Zhao Z, Li Y, Li L, Jiang Y, Cao Y, et al. Characterizations of the urate transporter, GLUT9, and its potent inhibitors by patch-clamp technique. *SLAS Discovery*. 2021;26:450–9.
- Nakamura M, Fujita K, Toyoda Y, Nakamura M, Fujita K, Toyoda Y, et al. Investigation of the transport of xanthine dehydrogenase inhibitors by the urate transporter ABCG2. *Drug Metab Pharmacokin*. 2018;33:77–81.
- Wu XH, Wang CZ, Wang SQ, Chao M, He Y, Zhang J, et al. Anti-hyperuricemia effects of allopurinol are improved by *Smilax riparia*, a traditional Chinese herbal medicine. *J Ethnopharmacol*. 2015;162:362–8.
- Sanguinetti MC, Jiang C, Curran ME, Keating MT. A mechanistic link between an inherited and an acquired cardiac arrhythmia: hERG encodes the  $I_{Kr}$  potassium channel. *Cell*. 1995;81:299–307.
- Helliwell RM. Recording hERG potassium currents and assessing the effects of compounds using the whole-cell patch-clamp technique. *Methods Mol Biol*. 2008;491:279–95.
- Kamiya K, Niwa R, Morishima M, Honjo H, Sanguinetti MC. Molecular determinants of hERG channel block by terfenadine and cisapride. *J Pharm Sci*. 2008;108:301–7.
- Tan PK, Liu S, Gunic E, Miner JN. Discovery and characterization of verinurad, a potent and specific inhibitor of URAT1 for the treatment of hyperuricemia and gout. *Sci Rep*. 2017;7:665.
- Gliozzi M, Malara N, Muscoli S, Mollace V. The treatment of hyperuricemia. *Int J Cardiol*. 2016;213:23–7.
- Taniguchi T, Ashizawa N, Matsumoto K, Saito R, Motoki K, Sakai M, et al. Pharmacological evaluation of dotinurad, a selective urate reabsorption inhibitor. *J Pharmacol Exp Ther*. 2019;371:162–70.
- Tan PK, Ostertag TM, Miner JN. Mechanism of high affinity inhibition of the human urate transporter URAT1. *Sci Rep*. 2016;6:34995.
- Woodward OM. ABCG2: the molecular mechanisms of urate secretion and gout. *Am J Physiol Ren Physiol*. 2015;309:F485–8.
- Miyata H, Takada T, Toyoda Y, Matsuo H, Ichida K, Suzuki H. Identification of febuxostat as a new strong ABCG2 inhibitor: potential applications and risks in clinical situations. *Front Pharmacol*. 2016;7:518.
- Qin Z, Wang S, Lin Y, Zhao Y, Yang S, Song J, et al. Antihyperuricemic effect of mangiferin aglycon derivative J99745 by inhibiting xanthine oxidase activity and urate transporter 1 expression in mice. *Acta Pharm Sin B*. 2018;8:306–15.
- Chen M, Ye C, Zhu J, Zhang P, Jiang Y, Lu X, et al. Bergenin as a novel urate-lowering therapeutic strategy for hyperuricemia. *Front Cell Dev Biol*. 2020;8:703.
- Torrallba KD, De Jesus E, Rachabattula S. The interplay between diet, urate transporters and the risk for gout and hyperuricemia: current and future directions. *Int J Rheum Dis*. 2012;15:499–506.
- Kedar E, Simkin PA. A perspective on diet and gout. *Adv Chronic Kidney Dis*. 2012;19:392–7.

36. Mehmood A, Zhao L, Wang C, Nadeem M, Raza A, Ali N, et al. Management of hyperuricemia through dietary polyphenols as a natural medicament: a comprehensive review. *Crit Rev Food Sci Nutr*. 2019;59:1433–55.
37. Major TJ, Dalbeth N, Stahl EA, Merriman TR. An update on the genetics of hyperuricaemia and gout. *Nat Rev Rheumatol*. 2018;14:341–53.
38. Auberson M, Stadelmann S, Stoudmann C, Seuwen K, Koesters R, Thorens B, et al. SLC2A9 (GLUT9) mediates urate reabsorption in the mouse kidney. *Pflug Arch*. 2018;470:1739–51.
39. Ruiz A, Gautschi I, Schild L, Bonny O. Human mutations in SLC2A9 (Glut9) affect transport capacity for urate. *Front Physiol*. 2018;9:476.
40. Kaufmann P, Torok M, Hanni A, Roberts P, Gasser R, Krahenbuhl S, et al. Mechanisms of benzarone and benzbromarone-induced hepatic toxicity. *Hepatology*. 2005;41:925–35.
41. Reinders MK, van Roon EN, Jansen TL, Delsing J, Griep EN, Hoekstra M, et al. Efficacy and tolerability of urate-lowering drugs in gout: a randomised controlled trial of benzbromarone versus probenecid after failure of allopurinol. *Ann Rheum Dis*. 2009;68:51–6.
42. Fleischmann R, Kerr B, Yeh LT, Suster M, Shen Z, Polvent E, et al. Pharmacodynamic, pharmacokinetic and tolerability evaluation of concomitant administration of lesinurad and febuxostat in gout patients with hyperuricaemia. *Rheumatol (Oxf)*. 2014;53:2167–74.
43. Hall J, Gillen M, Yang X, Shen Z. Pharmacokinetics, pharmacodynamics, and tolerability of concomitant administration of verinurad and febuxostat in healthy male volunteers. *Clin Pharmacol Drug Dev*. 2019;8:179–87.
44. Fleischmann R, Winkle P, Hall J, Valdez S, Liu S, Yan X, et al. Pharmacodynamic and pharmacokinetic effects and safety of verinurad in combination with febuxostat in adults with gout: a phase IIa, open-label study. *RMD Open*. 2018;4:e647.
45. Rizwan AN, Burckhardt G. Organic anion transporters of the SLC22 family: biopharmaceutical, physiological, and pathological roles. *Pharmacol Res*. 2007;24:450–70.
46. Yan N. Structural biology of the major facilitator superfamily transporters. *Annu Rev Biophys*. 2015;44:257–83.
47. Li DC, Nichols CG, Sala-Rabanal M. Role of a hydrophobic pocket in polyamine interactions with the polyspecific organic cation transporter OCT3. *J Biol Chem*. 2015;290:27633–43.
48. Lu J, Dalbeth N, Yin H, Li C, Merriman TR, Wei WH, et al. Mouse models for human hyperuricaemia: a critical review. *Nat Rev Rheumatol*. 2019;15:413–26.
49. Alghamdi YS, Soliman MM, Nassan MA. Impact of Lesinurad and allopurinol on experimental hyperuricemia in mice: biochemical, molecular and immunohistochemical study. *BMC Pharmacol Toxicol*. 2020;21:10.
50. Tan Y, Wang L, Gao J, Ma J, Yu H, Zhang Y, et al. Multiomics integrative analysis for discovering the potential mechanism of dioscin against hyperuricemia mice. *J Proteome Res*. 2020;20:645–60.
51. Chen M, Lu X, Lu C, Shen N, Jiang Y, Chen M, et al. Soluble uric acid increases PDZK1 and ABCG2 expression in human intestinal cell lines via the TLR4-NLRP3 inflammasome and PI3K/Akt signaling pathway. *Arthritis Res Ther*. 2018;20:20.
52. Anzai N, Miyazaki H, Noshiro R, Khamdang S, Chairoungdua A, Shin H, et al. The multivalent PDZ domain-containing protein PDZK1 regulates transport activity of renal urate-anion exchanger URAT1 via its C terminus. *J Biol Chem*. 2004;279:45942–50.
53. Srivastava S, Nakagawa K, He X, Kimura T, Fukutomi T, Miyauchi S, et al. Identification of the multivalent PDZ protein PDZK1 as a binding partner of sodium-coupled monocarboxylate transporter SMCT1 (SLC5A8) and SMCT2 (SLC5A12). *J Physiol Sci*. 2019;69:399–408.
54. Mandal AK, Mount DB. The molecular physiology of uric acid homeostasis. *Annu Rev Physiol*. 2015;77:323–45.
55. Yano H, Tamura Y, Kobayashi K, Tanemoto M, Uchida S. Uric acid transporter ABCG2 is increased in the intestine of the 5/6 nephrectomy rat model of chronic kidney disease. *Clin Exp Nephrol*. 2014;18:50–5.
56. Sekine T, Endou H. The mechanisms of urate transport in the kidney and the intestine. *Nihon Rinsho*. 1996;54:3237–42.
57. Koepsell H. The SLC22 family with transporters of organic cations, anions and zwitterions. *Mol Asp Med*. 2013;34:413–35.
58. Xu X, Li C, Zhou P, Jiang T. Uric acid transporters hiding in the intestine. *Pharm Biol*. 2016;54:3151–5.
59. Hoque KM, Dixon EE, Lewis RM, Allan J, Gamble GD, Phipps-Green AJ, et al. The ABCG2 Q141K hyperuricemia and gout associated variant illuminates the physiology of human urate excretion. *Nat Commun*. 2020;11:2767.
60. DeBosch BJ, Kluth O, Fujiwara H, Schurmann A, Moley K. Early-onset metabolic syndrome in mice lacking the intestinal uric acid transporter SLC2A9. *Nat Commun*. 2014;5:4642.